

ON GENERALIZED FINITE ELEMENT METHOD'S NUMERICAL STABILITY PRESERVATION

Daniel C. Sales¹, Sergio P. B. Proença¹

¹*Dept. of Structural Engineering, São Carlos School of Engineering, University of São Paulo
Avenida Trabalhador São Carlense, 400, 13566-590, São Paulo/São Carlos, Brazil
csalesdaniel@usp.br, persival@sc.usp.br*

Abstract. The Generalized Finite Element Method (GFEM) proposes the expansion of FEM's approximation space by combining Partition of Unity (PU) functions with enrichment functions. Such combination provides locally better capacity to approximate the desired solution. PU functions combine local approximations, forming the corresponding global approximation. The Galerkin method is employed, leading to a system of equations to be solved for global nodal parameters. However, it is important that the extended approximation space is linearly independent, as to not jeopardize GFEM's system's conditioning which could lead to inaccurate results. Recent developments propose alternatives for preserving the solving system's linear independence, improving its conditioning. This work offers new contributions in two manners. On one hand, a new set of PU functions to compose the enriched space is explored. On the other hand, the Singular Value Decomposition (SVD) methodology is explored to obtain adequate solutions even in the presence of linear dependencies. Examples that normally lead to dependencies are explored, emphasizing the advantages of the strategies. It is shown that GFEM's system's conditioning is close to FEM's while employing the new PU. Also, SVD's efficiency for solving the system disregarding its dependencies is demonstrated, adding robustness to the most conventional versions of the method.

Keywords: Generalized Finite Element Method, Higher Order Polynomial PU, Singular Value Decomposition, Scaled Condition Number.

1 Introduction

The Generalized Finite Element Method (GFEM) has shown potential in a broad set of applications, such as fluid-structure interaction, crack and shear band simulations, as seen in Belytschko et al. [1]. A GFEM major advantage lies in its excellent convergence properties, achieved through the approximation's space expansion, combining special enrichment functions with PU sets to locally mimic solution's expected behavior while maintaining conformity in the global approximation. However, the unrestricted expansion of the approximation space may lead to ill conditioned solving systems, as observed in many works, such as Strouboulis et al. [2] and Gupta et al. [3].

Many studies were developed addressing this issue, e.g. Zhang et al. [4], Zhang et al. [5], Babuška and Banerjee [6] and Cui and Zhang [7], with different solutions and applications. In this paper, we offer contributions in two different aspects. First, we explore the use of a high order polynomial PU in the construction of the enriched space as a way to improve system's conditioning. On the other hand, we examine a different way to solve GFEM's linear systems even when they are ill conditioned.

2 Model Problem Formulation

Let $\bar{\Omega} = \Omega \cup \partial\Omega \in \mathbb{R}^2$ be a domain of linear elastic behavior. The governing equations of the Boundary Value Problem (BVP), namely equilibrium, constitutive and compatibility, are respectively given by:

$$\nabla \cdot \boldsymbol{\sigma} = \mathbf{0}, \quad \boldsymbol{\sigma} = \mathbf{C} : \boldsymbol{\epsilon}, \quad \boldsymbol{\epsilon} = \nabla_s \mathbf{u} \quad \text{in } \Omega \quad (1)$$

where $\boldsymbol{\sigma}$, \boldsymbol{C} and $\boldsymbol{\epsilon}$ represent the Cauchy's stress, Hooke's and small strain tensors, respectively, while \mathbf{u} is the vector-valued displacement field.

Neumann and Dirichlet boundary conditions are then imposed on $\partial\Omega$ as follows:

$$\boldsymbol{\sigma} \cdot \mathbf{n} = \bar{\mathbf{t}} \quad \text{on } \partial\Omega^\sigma, \quad \mathbf{u} = \bar{\mathbf{u}} \quad \text{on } \partial\Omega^u \quad (2)$$

where \mathbf{n} is the outward normal vector to $\partial\Omega$, $\bar{\mathbf{t}}$ and $\bar{\mathbf{u}}$ denote prescribed traction and displacement, respectively. Also, $\partial\Omega = \partial\Omega^\sigma \cup \partial\Omega^u$ and $\partial\Omega^\sigma \cap \partial\Omega^u = \emptyset$. Once crack is present, crack surfaces are assumed free of traction.

Through the weak formulation and Galerkin's method, a finite dimensional approximation \mathbf{u}_h of \mathbf{u} can be found by solving the following problem:

Find $\mathbf{u}_h \in \mathcal{S}(\Omega) \subset \mathcal{E}(\Omega)$ such that $\forall \mathbf{v}_h \in \mathcal{S}(\Omega)$

$$\begin{aligned} B(\mathbf{u}_h, \mathbf{v}_h) &= F(\mathbf{v}_h), \quad \text{with} \\ B(\mathbf{u}_h, \mathbf{v}_h) &= \int_{\Omega} \boldsymbol{\sigma}(\mathbf{u}_h) : \boldsymbol{\epsilon}(\mathbf{v}_h) dA, \quad F(\mathbf{v}_h) = \int_{\partial\Omega} \bar{\mathbf{t}} \cdot \mathbf{v}_h ds \end{aligned} \quad (3)$$

The above mentioned $\mathcal{S}(\Omega)$ is the trial/test functions space that provides a discretization of the energy space $\mathcal{E}(\Omega)$ with energy norm $\|\cdot\|_{\mathcal{E}(\Omega)} = \sqrt{B(\cdot, \cdot)}$. Equation 3 leads to a linear system of equations which can be solved for the parameters appearing in the approximate solution, also known as degrees of freedom (DOFs). It is observed that the approximation space $\mathcal{S}(\Omega)$ is hereby constructed through the GFEM/SGFEM.

3 On GFEM/SGFEM Shape Functions and the Partitions of Unity Involved

The GFEM is a Galerkin Method that proposes the expansion of the conventional FEM approximation space, \mathcal{S}_{FEM} , through special functions called *enrichment functions*. This expansion allows to take advantage of a-priori knowledge about the problem's solution by exploring special functions that better mimic locally its behavior. To build the GFEM's approximation, \mathbf{u}_h^{GFEM} , these special functions are multiplied by conventional FEM shape functions, Lagrangian linear or bilinear, which are Partitions of Unity (PU).

Let $\{(x_i, y_i) : i \in I_h\}$ be the set of nodes in the finite element mesh adopted in the discretization, where h is indicative of the elements' size and I_h is the set of nodal indexes. Moreover, ϕ_i is the PU hat-function attached to node i with support cloud ω_i (set of elements sharing this node). Also, let L_j^i denote the j -th component, $1 \leq j \leq n_i$, of the enrichment functions' vector \mathbf{L}^i on node i , with $L_1^i = 1$. The GFEM's global approximation function is then given by:

$$\mathbf{u}_h = \sum_{i \in I_h} \sum_{j=1}^{n_i} \phi_i L_j^i \mathbf{b}_j^i = \sum_{i \in I_h} \phi_i \mathbf{a}_i + \sum_{i \in I_h} \sum_{j=2}^{n_i} \phi_i L_j^i \mathbf{b}_j^i = \mathbf{u}_h^{FEM} + \mathbf{u}_h^{ENR} \quad (4)$$

where $\mathbf{b}_j^i \in \mathbb{R}^2$ represents the discretization's parameters, or DOFs, $\mathbf{a}_i = \mathbf{b}_1^i$ and \mathbf{u}_h^{FEM} , \mathbf{u}_h^{ENR} are FEM's approximation and the enriched part of GFEM's approximation, respectively.

Despite its excellent convergence properties, GFEM's conditioning is generally worse than the FEM one. Addressing this issue, Babuška and Banerjee [6] proposed a stable GFEM (SGFEM) based on a simple modification of the enrichment functions, consisting on subtracting its linear interpolant as follows:

$$\bar{L}_j^i = L_j^i - \mathcal{I}_{\omega_i} L_j^i, \quad \mathcal{I}_{\omega_i} L_j^i(x, y) = \sum_{k \in I_h} \phi_k(x, y) L_j^i(x_k, y_k) \quad (5)$$

where $\mathcal{I}_{\omega_i} L_j^i(x, y)$ is the finite element interpolant of $L_j^i(x, y)$.

It is shown and exemplified in Babuška and Banerjee [6] that this modification improves the conditioning and also does not require any special treatments for blending elements.

Nevertheless, it was shown in Zhang et al. [4] with polynomial enrichments that it does not fully prevent linear dependencies. The solution proposed then was employing a different PU, for instance the flat-top PU, to

build the enrichment space. Sato et al. [8] extended the flat-top PU formulation to two-dimensional domains with quadrilateral elements, achieving good system conditioning even with polynomial enrichments. Next, Ramos et al. [9], in the context of a SGFEM for elasticity crack problems, presented good conditioning and convergence results through enrichment spaces built partly with the use of non hat-function PUs, namely flat-top PU and a trigonometric PU. Recently, in Cui and Zhang [7], a higher order polynomial PU was employed in a similar context to Ramos et al. [9]. Following Cui and Zhang [7], in this paper, we explore the high order PU along with polynomial enrichments seeking for convergence improvement, as well as for stability control.

The higher order polynomial PU is a set of Hermite interpolation polynomials which, for a one-dimensional master element $[0, 1]$ and its generalization to a two-dimensional quadrilateral master element $[0, 1] \times [0, 1]$ through a tensorial product, respectively, is given by:

$$\begin{aligned} Q_0^1 &= (1 - \xi)^2(1 + 2\xi), & Q_1^1 &= \xi^2(3 - 2\xi) \\ Q_{mn}^1(\xi, \eta) &= Q_m^1(\xi)Q_n^1(\eta), & m, n &= 0, 1 \end{aligned} \quad (6)$$

4 Singular Value Decomposition

Despite the presence of linear dependencies in the system of equations, as the BVP is well posed, the solution is unique, i.e., the resulting approximate solution should always be the same if the system is properly solved, without sensible influence of roundoff errors. Different strategies have been suggested for solving ill conditioned GFEM's systems such as the iterative algorithm presented in Strouboulis et al. [2] and the multifrontal sparse Gaussian elimination in Duff and Reid [10].

We hereby present another strategy for solving such systems, based on the relation between Singular Value Decomposition (SVD) of the stiffness matrix \mathbf{K} and its Moore–Penrose inverse. First, we set a minimum value for computed singular values, λ , used in the solution. Then, compute r singular values greater than λ and their related right and left singular vectors. Eckart-Young theorem states that the best r -ranked approximation to \mathbf{K} is given through SVD by:

$$\mathbf{K} \approx \mathbf{U}_{nDOF \times r} \mathbf{\Sigma}_{r \times r} (\mathbf{V}^T)_{r \times nDOF} = \mathbf{A}_{nDOF \times nDOF} \quad (7)$$

$nDOF$ is the total number of discretization's DOFs, the columns of $\mathbf{U}_{nDOF \times r}$ and $\mathbf{V}_{nDOF \times r}$ are the left and right singular vectors, respectively, $\mathbf{\Sigma}_{r \times r}$ is a diagonal matrix with the r singular values and $\mathbf{A}_{nDOF \times nDOF}$ is the approximate matrix. Also, $\mathbf{U}_{nDOF \times r} = \mathbf{V}_{nDOF \times r}$ because \mathbf{K} is symmetric, so only one of them needs to be computed.

The approximate matrix's Moore–Penrose inverse is then computed as follows:

$$\mathbf{A}_{nDOF \times nDOF}^+ = \mathbf{V}_{nDOF \times r} \mathbf{\Sigma}_{r \times r}^+ (\mathbf{U}^T)_{r \times nDOF} \quad (8)$$

where $\mathbf{\Sigma}_{r \times r}^+$ is formed, in this case, by replacing every diagonal entry of $\mathbf{\Sigma}_{r \times r}$ by its reciprocal. Finally, the approximate solution is found pre-multiplying the independent vector by $\mathbf{A}_{nDOF \times nDOF}^+$. In this paper, we set $\lambda = 10^{-12}$, an extremely low value, so only non null singular values, taking the machine epsilon into account, are computed and the original system's solution is recovered.

5 Numerical Examples

The results herein presented were obtained from the problem shown in Fig. 1a. It consists of a two-dimensional edge crack square panel, with a crack line Γ_C and a crack tip C . The Neumann boundary conditions applied correspond to the first term of the pure Mode I solution's asymptotic expansion in the neighborhood of a crack, Szabó and Babuška [11] for reference. The crack surface is traction-free. Dirichlet boundary conditions were applied to prevent rigid body motion, as the load is self-balanced, so the stiffness matrix is not singular unless linear dependencies appear in the enriched approximation space $\mathcal{S}(\Omega)$. Plane strain condition was assumed. Young Modulus $E = 1.0$ and Poisson's ratio $\nu = 0.3$ were adopted.

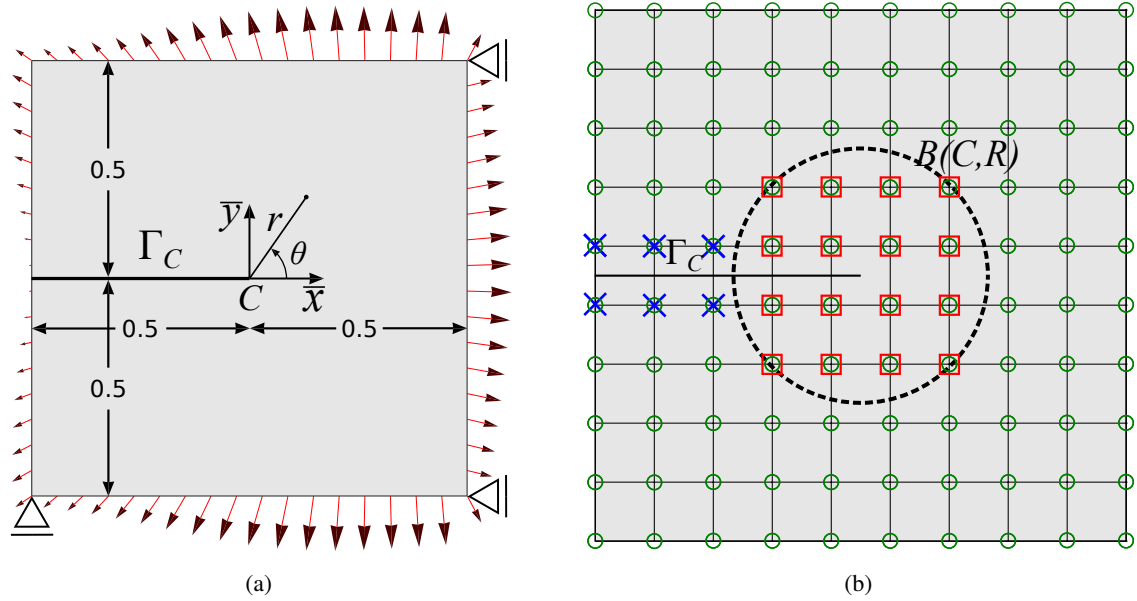


Figure 1. (a) Edge crack panel and (b) enrichment strategy. Nodes marked with “□” are enriched by singular functions, “X” nodes by linear Heaviside functions and “o” nodes by polynomial functions.

Figure 1b shows an example of a typical mesh used in the simulations and enrichment distributed at the nodes. Quadrilateral elements with $h = \frac{1}{2^{(i+1)+1}}$, $i = 1, 2, \dots, 6$ were employed in structured grids.

The singular enrichment functions present in the discretization are given by:

$$\begin{aligned} L^{S,\bar{x}}(r, \theta) &= \sqrt{r} \left\{ \left(\kappa - \frac{1}{2} \right) \cos \frac{\theta}{2} - \frac{1}{2} \cos \frac{3\theta}{2}, \left(\kappa + \frac{3}{2} \right) \sin \frac{\theta}{2} + \frac{1}{2} \sin \frac{3\theta}{2} \right\} \\ L^{S,\bar{y}}(r, \theta) &= \sqrt{r} \left\{ \left(\kappa + \frac{1}{2} \right) \sin \frac{\theta}{2} - \frac{1}{2} \sin \frac{3\theta}{2}, \left(\kappa - \frac{3}{2} \right) \cos \frac{\theta}{2} + \frac{1}{2} \cos \frac{3\theta}{2} \right\} \end{aligned} \quad (9)$$

where (r, θ) is the polar coordinate system defined on the crack's tip C and $\kappa = (3 - 4\nu)$. $L^{S,\bar{x}}$ and $L^{S,\bar{y}}$ are used to expand the approximation space along the local directions \bar{x} and \bar{y} , respectively, resulting in four additional DOFs per node. These enrichment functions are capable of representing the solution's singular behavior near C and are discontinuous in Γ_C . They were derived from the Modes I and II elasticity crack solutions and first used in Oden and Duarte [12] and Duarte et al. [13]. Coordinate system transformations are used in their implementation.

Linear Heaviside functions set is defined as follows:

$$\mathbf{L}^{LH}(x, y) = \left\{ H, H \frac{x - x_i}{h}, H \frac{y - y_i}{h} \right\}, \quad H(x, y) = \begin{cases} 1, & Z(x, y) \geq 0 \\ -1, & Z(x, y) < 0 \end{cases} \quad (10)$$

where $Z(x, y) = 0$ is the crack line equation. This set of functions is used to represent displacement discontinuity along Γ_C .

The enrichment strategy herein adopted for the singular and linear Heaviside functions follows Gupta et al. [3] and Zhang et al. [5] while delivering optimal convergence order $\mathcal{O}(h)$ and stiffness matrix conditioning close to FEM's when applied to both GFEM and SGFEM. The *geometric enrichment* strategy is employed for singular functions, therefore nodes in a ball $B(C, R)$ with $R = 0.25$ around the crack tip are enriched. Elements crossed by the crack line have its nodes that are not in $B(C, R)$ enriched with the Linear Heaviside set. The singular and Linear Heaviside nodes set, I_S and I_{LH} respectively, are given by:

$$I_S = \{i \in I_h : (x_i, y_i) \in B(C, R)\} \text{ and } I_{LH} = \{i \in I_h : (x_i, y_i) \in e_s \text{ and } e_s \cap \Gamma_C \neq \emptyset\} \setminus I_S; \quad (11)$$

where e_s is the set of elements intercepted by the crack Γ_C .

Aiming at higher order convergence, we expand the approximation space with the following shifted polynomial functions, applied to every node i of the discretization:

$$\mathbf{L}_i^{p=2}(x, y) = \left\{ \frac{(x - x_i)}{h_i}, \frac{(y - y_i)}{h_i}, \frac{(x - x_i)^2}{h_i^2}, \frac{(x - x_i)(y - y_i)}{h_i^2}, \frac{(y - y_i)^2}{h_i^2} \right\} \quad (12)$$

We observe that the modification suggested in Babuška and Banerjee [6] is not adopted for the subset $\mathbf{L}_i^{p=1}$ as the functions would be nullified.

Convergence analysis presented in this paper are based on the relative error in the energy norm, defined as:

$$\epsilon_h = \frac{\|\mathbf{u} - \mathbf{u}_h\|_{\mathcal{E}(\Omega)}}{\|\mathbf{u}\|_{\mathcal{E}(\Omega)}} \quad (13)$$

where \mathbf{u} is the known exact solution of the problem.

Moreover, system's conditioning analysis were controlled using the scaled condition number (SCN) $\mathfrak{K}(\mathbf{K})$ as indicator, given by:

$$\mathfrak{K}(\mathbf{K}) := \kappa_2(\hat{\mathbf{K}}) = \kappa_2(\mathbf{D}\hat{\mathbf{K}}\mathbf{D}), \quad \mathbf{D}_{ii} = \mathbf{K}_{ii}^{-1/2} \quad (14)$$

where \mathbf{D} is a diagonal matrix and $\kappa_2(\mathbf{A})$ is the condition number of \mathbf{A} .

5.1 Higher order polynomial PU

In order to control the tendency to loss of stability induced by polynomial enrichment, the following approximation, here referred as SGFEM_{HOP}, is built particularly multiplying polynomial enrichment functions by Hermitian polynomial PU:

$$\begin{aligned} \mathbf{u}_h = & \sum_{i \in I_h} \phi_i \mathbf{a}_i + \sum_{i \in I_{LH}} \sum_{j=1}^3 \phi_i \left(L_j^{LH} - \mathcal{I}_{\omega_i} L_j^{LH} \right) \mathbf{b}_j^i + \sum_{i \in I_S} \sum_{j=1}^2 \phi_i \left(L_j^S - \mathcal{I}_{\omega_i} L_j^S \right) \mathbf{c}_j^i + \\ & \sum_{i \in I_h} \sum_{j=1}^2 Q_i^1(L_i^{p=1})_j \mathbf{d}_j^i + \sum_{i \in I_h} \sum_{j=1}^3 Q_i^1 \left((L_i^{p=2} \setminus L_i^{p=1})_j - \mathcal{I}_{\omega_i} (L_i^{p=2} \setminus L_i^{p=1})_j \right) \mathbf{e}_j^i \end{aligned} \quad (15)$$

It is noted that the approximation is vector-valued and different singular functions are used in each direction, according to eq. (9).

Figure 2 shows a comparison of results obtained with different methods described in this paper. It is noted that the conditioning's increase rate is $\mathcal{O}(h^{-2})$ in the SGFEM_{HOP}, same order as the one provided by FEM, while GFEM and SGFEM yield singular systems. This can be explained as linear dependencies between the FEM's approximation space and the polynomial functions enrichments are eliminated through the use of a different PU. Such behavior is coherent with what has been shown in Zhang et al. [4], Sato et al. [8] and Ramos et al. [9]. Despite the conditioning improvement, error convergence order obtained using SGFEM_{HOP} was initially subpar in comparison to SGFEM and GFEM. The reason for such behavior was detected later to be error concentrations observed in the corner elements of the mesh. So a new modification was proposed, using FEM's *hat-functions* as PU for polynomial functions enrichments on corner nodes, SGFEM_{HOP}^{MD}. With this modification, as shown in Fig. 1 a quadratic convergence order $\mathcal{O}(h^2)$ was recovered along with conditioning growth $\mathcal{O}(h^{-2})$.

5.2 Singular Value Decomposition

In this section we present results regarding the methodology described in Section §4. Figure 3a compares the relative error in the energy norm obtained from different solution methods. The iterative procedure described

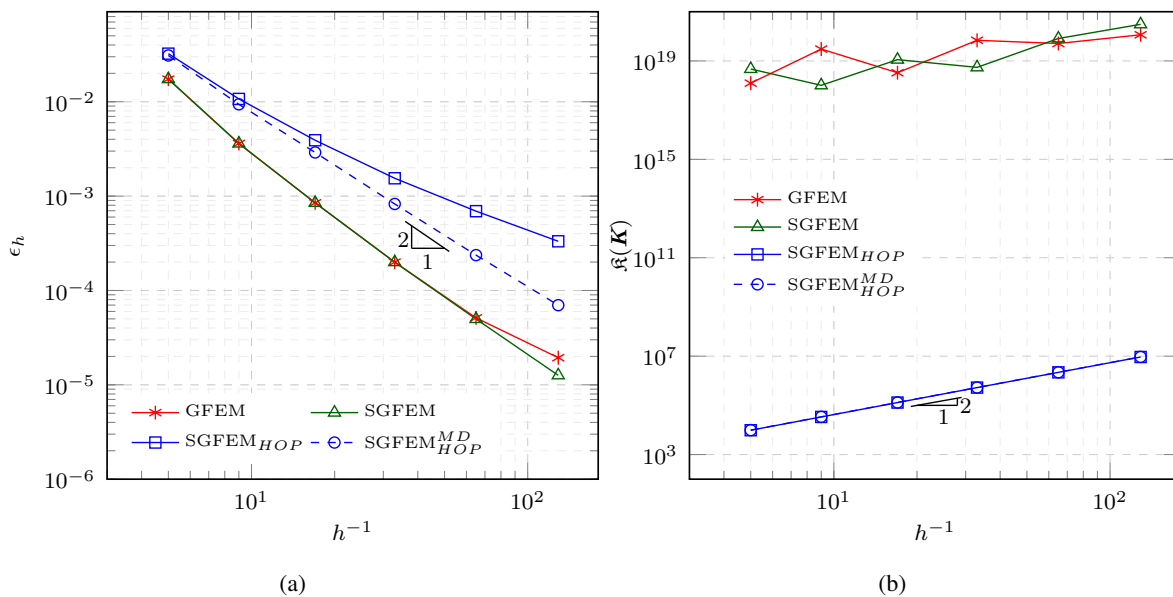


Figure 2. Higher order polynomial PU results: (a) Relative error in the energy norm convergence and (b) Scaled condition number growth.

in Strouboulis et al. [2] was adopted in the SGFEM curve, while SGFEM_{SVD}'s curve comes from the aforementioned methodology. Both methods yield practically equivalent solutions. It is observed from Fig. 3b that the solving system is singular, hence really high SCN, taking into account the machine epsilon. Nonetheless, SVD was able to deliver good results.

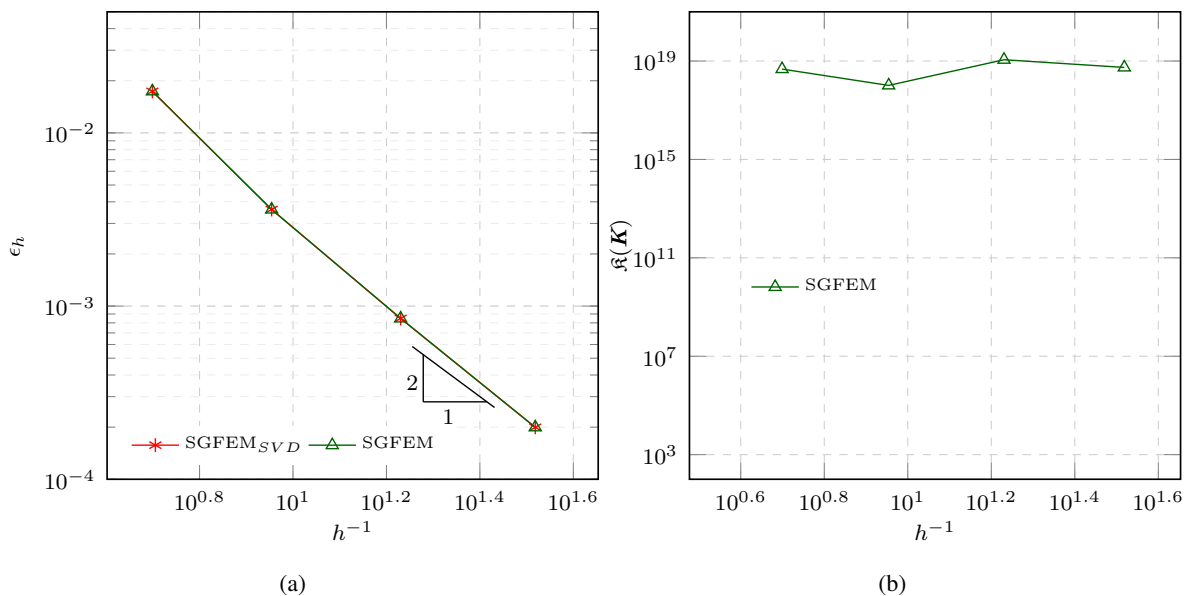


Figure 3. SVD results: (a) Relative error in the energy norm convergence and (b) Scaled condition number growth.

Finally, Table 1 addresses quite interesting results related to the matrix's rank, which is equal to the number of singular values and vectors computed for the solution, along with its nullity. It's observed that the nullity relatively decreases with mesh refinement. Similar behavior was also noted in Strouboulis et al. [2].

Table 1. Null singular values behavior

i	Number of DOFs	Rank	Rank %	Nullity %
1	472	398	84%	16%
2	1300	1176	90%	10%
3	4156	3932	95%	5%
4	14812	14388	97%	3%

6 Conclusions

Through the investigations presented in this paper, it is shown that the employment of the higher order polynomial PU in combination with polynomial enrichment functions enables for higher order convergence while maintaining good system conditioning. Also, the SVD methodology was explored for solving the singular or almost singular systems herein studied, providing accurate solutions despite existence of dependences. However, high computational cost can be involved with mesh refinement. In a future research, investments on computational efficiency improvement are going to be done aiming to better explore SVD advantages.

Acknowledgements. The authors would like to acknowledge the support of University of São Paulo (USP) and the financial support from Coordination for the Improvement of Higher Education Personnel (CAPES).

Authorship statement. The authors hereby confirm that they are the sole liable persons responsible for the authorship of this work, and that all material that has been herein included as part of the present paper is either the property (and authorship) of the authors, or has the permission of the owners to be included here.

References

- [1] Belytschko, T., Gracie, R., & Ventura, G., 2009. A review of extended/generalized finite element methods for material modeling. *Modelling and Simulation in Materials Science and Engineering*, vol. 17, n. 4.
- [2] Strouboulis, T., Babuška, I., & Copps, K., 2000. The design and analysis of the Generalized Finite Element Method. *Computer Methods in Applied Mechanics and Engineering*, vol. 181, n. 1-3, pp. 43–69.
- [3] Gupta, V., Duarte, C. A., Babuška, I., & Banerjee, U., 2013. A stable and optimally convergent generalized FEM (SGFEM) for linear elastic fracture mechanics. *Computer Methods in Applied Mechanics and Engineering*, vol. 266, pp. 23–39.
- [4] Zhang, Q., Banerjee, U., & Babuška, I., 2014. Higher order stable generalized finite element method. *Numerische Mathematik*, vol. 128, n. 1, pp. 1–29.
- [5] Zhang, Q., Babuška, I., & Banerjee, U., 2016. Robustness in stable generalized finite element methods (SGFEM) applied to Poisson problems with crack singularities. *Computer Methods in Applied Mechanics and Engineering*, vol. 311, pp. 476–502.
- [6] Babuška, I. & Banerjee, U., 2012. Stable Generalized Finite Element Method (SGFEM). *Computer Methods in Applied Mechanics and Engineering*, vol. 201-204, pp. 91–111.
- [7] Cui, C. & Zhang, Q., 2020. Stable generalized finite element methods for elasticity crack problems. *International Journal for Numerical Methods in Engineering*, vol. 121, n. 14, pp. 3066–3082.
- [8] Sato, F. M., Neto, D. P., & Proença, S. P. B., 2018. Numerical experiments with the generalized finite element method based on a flat-top partition of unity. *Latin American Journal of Solids and Structures*, vol. 15.
- [9] Ramos, C. S., Bento, M. H. C., & Proença, S. P. B., 2019. A stable and improved version of the gfem for the analysis of problems in elastic linear fracture. In *Proceedings of the XL Ibero-Latin-American Congress on Computational Methods in Engineering*. ABMEC.
- [10] Duff, I. S. & Reid, J. K., 1983. The Multifrontal Solution of Indefinite Sparse Symmetric Linear. *ACM Transactions on Mathematical Software (TOMS)*, vol. 9, n. 3, pp. 302–325.
- [11] Szabó, B. & Babuška, I., 1991. *Finite Element Analysis*. John Wiley and Sons.
- [12] Oden, J. T. & Duarte, C. A., 1997. Cloud, Cracks and FEMs. *Recent Developments in Computational and Applied Mechanics*.
- [13] Duarte, C. A., Babuška, I., & Oden, J. T., 2000. Generalized finite element methods for three-dimensional structural mechanics problems. *Computers and Structures*, vol. 77, n. 2, pp. 215–232.